Available online at www.sciencedirect.com
SCIENCE DIRECT®

Journal of the European Ceramic Society 23 (2003) 2343–2349
www.elsevier.com/locate/jeurceramsoc

Phase assemblages of (Ca,Mg)-α-sialon ceramics derived from an α-sialon powder prepared by SHS

Jiuxin Jiang[a], Peiling Wang[a,*], Weiwu Chen[a], Hanrui Zhuang[b], Yibing Cheng[c], Dongsheng Yan[a]

[a]*The State Key Lab of High Performance Ceramics and Superfine Microstructure, Shanghai Institute of Ceramics, Chinese Academy of Science, Shanghai 200050, PR China*
[b]*The Center of Structural Ceramics, Shanghai Institute of Ceramics, Chinese Academy of Science, Shanghai 200050, PR China*
[c]*School of Physics and Materials Engineering, Monash University, Clayton, Victoria 3800, Australia*

Received 22 September 2002; received in revised form 2 January 2003; accepted 13 January 2003

Abstract

(Ca,Mg)-α-sialon powders were previously [J. Mater. Chem. 12 (2002) 1199] prepared by Self-propagating high-temperature synthesis (SHS) technology using slag as a raw material (abbreviated as Slag α-sialon powder). In this study, phase assemblages of the Slag α-sialon samples hot-pressed from 1450 to 1700 °C were investigated. Results indicated that α-sialon was the main crystalline phase in the whole sintering process, however, a small amount of β-sialon appeared in the samples sintered at 1500 °C and above. In addition, the SHS technique was also used to prepare α-sialon powders using chemical agents as raw materials (named Chem α-sialon). Samples made from the Chem α-sialon powder were hot-pressed under the same conditions for a comparison. Similar phase assemblages were obtained for the samples starting from Chem α-sialon powders, except for even more amount of βsialon phase contained. Material with a single α-sialon phase could be got in both samples when 10 wt.% additional slag and $CaCO_3$ were introduced into the Slag α-sialon and Chem α-sialon starting powders respectively.

Keywords: Phase development; SHS; Sialons; Slag

1. Introduction

Si_3N_4-based sialon ceramics possess outstanding properties, such as super-wear and corrosion resistance, good anti-oxidation and thermal shock behavior, as well as high strength and hardness up to high temperature.[2] These make sialon ceramics be applied not only at high temperature and corrosive environments in metallurgy and chemical industries, but also as cutting tools and bearings. However, sialon ceramics have not been extensively applied even after twenty years' development, mainly because its high cost, including the cost of powder fabrication and ceramic processing, is far beyond the market expectation. To reduce the cost, sialon powders made by carbothermal reduction and nitridation (CRN) method using cheap raw materials, such as clay,[3,4] kaolinite[5] and montmorillonite [6] have been investigated.

The self-propagating high-temperature synthesis (SHS) technique was firstly reported by Merzhanov in 1972.[7] The SHS process does not require a high-temperature furnace and the reactions can be completed within seconds instead of hours or days as in the CRN process. The advantages of high productivity and low energy consumption have made SHS a favorable technique to synthesize materials,[8–10] such as carbide, nitride, boride, $MoSi_2$, and to recycle industrial wastes.[11–13] It was reported in our previous paper[1] that (Ca,Mg)-α-sialon powder was successfully synthesized for the first time by the SHS technology using slag as a raw material. There is an advantage of the synthesis of α-sialon powder using slag as the major starting material because the composition of slag, consisting mainly of CaO, SiO_2, Al_2O_3 and MgO, can be easily tailored to form α-sialon if extra nitrogen is incorporated.

* Corresponding author. Tel.: +86-21-524-12324; fax: +86-21-524-13122.
E-mail address: plwang@sunm.shcnc.ac.cn (P. Wang).

0955-2219/03/$ - see front matter © 2003 Elsevier Ltd. All rights reserved.
doi:10.1016/S0955-2219(03)00043-8

In the conventional sintering of α-sialon ceramics, α-Si_3N_4, AlN and oxides are used as starting materials. The reaction between the oxides existing on the surfaces of nitrides and the oxide additives can produce a eutectic liquid phase at a certain temperature depending on the composition. With the increase of sintering temperature, the amount of liquid phase increases and α-Si_3N_4 dissolves in the liquid. The α-sialon phase forms when the substitution of Al–O and Al–N bonds for Si–N bonds occurs followed by the stabilizing metal ions absorbed into the sialon structure, which precipitates from the transient liquid phase when its concentration reaches a limit.[14] The formation of Slag α-sialon completes in seconds and cools very rapidly. This could result in the Slag α-sialon phase in a non-equilibrium/meta-stability state.[1] The meta-stability of α-sialon powders may have better sinter-ability. This feature makes the SHS α-sialon powders especially appealing for production, as α-sialon is known to have poor sinter-ability. On the other hand, it is expected that the sintering behavior of α-sialon ceramics made from the Slag α-sialon powder would be different from that of the materials made from the synthesized chemicals. It is therefore necessary to explore the reaction sequence of Slag α-sialon ceramics. The purpose of the present work is to study the densification and phase assemblages of Slag α-sialon samples hot-pressed at different temperatures. As a comparison, (Ca,Mg) α-sialon powders of the same composition as the Slag α-sialons were also synthesized by SHS but using chemical reagents as starting materials.

2. Experimental

The general formula of (Ca,Mg)-α-sialon is represented as $(Ca,Mg)_xSi_{12-(m+n)}Al_{(m+n)}O_nN_{16-n}$, where m(Si–N) are substituted by m(Al–N), n(Si–N) by n(Al–O), and the valence discrepancy introduced is compensated by Ca and Mg. The composition of (Ca,Mg)-α-sialon used for SHS synthesis was located on the tie line Si_3N_4–Ca(Mg)O:3AlN with a formula of $(Ca,Mg)_xSi_{12-3x}Al_{3x}O_xN_{16-x}$, i.e. $x=m/2=n$ and designed as $Ca_{0.71}Mg_{0.23}Si_{9.18}Al_{2.82}O_{0.94}N_{15.06}$ based on the composition of slag.[1] Starting materials for synthesizing Slag α-sialon and Chem α-sialon powders by SHS included slag (Baoshan Steel Inc., Shanghai, China), Si_3N_4 (UBE E10, Japan, 2 wt.%O), AlN (Wuxi, China, 1.3 wt.%O), Si (Si > 98 wt.%, 30 μm), Al (Al > 98wt.%, 25 μm), $CaCO_3$ (> 99 wt.%) and MgO (> 98 wt.%). The well-mixed powders were put into a graphite crucible and covered with a top layer of titanium powders. A tungsten heating coil was connected to ignite the Ti powder, which then induced the spontaneous SHS process. Before starting the ignition, nitrogen with 50 MPa pressure was passed into the container. The whole process was held in a sealed cabin with a high pressure of N_2 and the reaction can be approximately expressed as:

$$0.71CaO + 0.23MgO + 9.18Si + 7.53N \rightarrow Ca_{0.71}Mg_{0.23}Si_{9.18}Al_{2.82}O_{0.94}N_{15.06} \quad (1)$$

α-sialon powders synthesized by SHS were attrition milled for 24 h. Subsequent ball milling of the synthesized Slag α-sialon powder and Chem α-sialon powder with additional slag and $CaCO_3$ respectively were carried out for 2 h.

The dried Slag α-sialon powders were hot-pressed in flowing N_2 at temperatures ranging from 1450 to 1700 °C in an interval of 50 °C for 1 h respectively under a pressure of 20 MPa in a graphite furnace. The hot-pressing temperatures of Chem α-sialon were 1450, 1550, 1650 and 1700 °C for 1 h. The compositions used for extra slag/$CaCO_3$ respectively added into Slag/Chem α-sialon powders are listed in Table 1. The mixtures of Slag α-sialon plus slag and Chem α-sialon plus $CaCO_3$ were hot-pressed at 1650 and 1550 °C for 1 h, respectively. To make the microstructure of sintered samples by back-scattered mode under scanning electron microscope (SEM), 2.0 wt.% La_2O_3 was added into some of the Slag α-sialon and Chem α-sialon samples in order to enhance atomic contrast of their back scattered SEM images. The reason to add La_2O_3 as a "dye" is because La could not enter the α-sialon structure under the present sintering condition. The compositions of Slag/Chem α-sialon powders with added La_2O_3 are tabulated in Table 1 too. The two mixtures were hot-pressed at 1700 and 1650 °C for 1 h respectively.

The bulk densities of the samples were measured according to the Archimedes principle. Phase characterization of hot-pressed samples was based on X-ray diffraction data from a Guinier-Hägg camera using Cu $K_{\alpha 1}$ radiation and Si as an internal standard. The measurement of X-ray film and refinement of lattice parameters were completed by a computer-linked line scanner (LS-18) system[15] and SCANPI, PIRUM programs. The microstructure observation was performed under scanning electron microscope (SEM, EPMA-8705) equipped with an energy dispersive spectrometer (Oxford/LINK ISIS 3.00). The contents of some elements in SHS-ed slag α-sialon powder was measured by ICP-AES (inductively coupled plasma-atomic emission spectrum) technique.

Table 1
Compositions used for extra slag/CaO/La_2O_3 added into Slag/Chem α-sialon powders

Mixtures	Composition (wt.%)				
	Slag α-sialon	Chem α-sialon	Slag	CaO	La_2O_3
I	90		10		
II		93		7	
III	98				2
IV		98			2

3. Results and discussion

3.1. Characteristics of Slag and Chem α-sialon powders derived by SHS

The XRD patterns of Slag α-sialon and Chem α-sialon powders are shown in Fig. 1. As seen from the figure, the final product of both powders is a single α-sialon phase, indicating that the SHS technique can synthesize α-sialon powder not only from stoichiometrical composition, but also from industrial wastes through proper compositional tailoring.

It is expected that the α-sialon phase and its related phase assemblages prepared by SHS and the conventional heating processes, such as hot-pressing and pressureless sintering, should have distinct characteristics. It was found that monolithic (Ca,Mg)-α-sialon is difficult to form from the compositions located on the tie line Si_3N_4–Ca(Mg)O:3AlN by conventional hot-pressing as an AlN-polytypoid phase usually co-exists with the α-sialon phase when the x value in the composition is higher than 0.6.[16,17] In contrast, no crystalline phases other than the α-sialon were observed in the SHS-ed powder. This could be attributed to the high temperature and accelerated mass diffusion, enabling more complete reactions for the formation of α-sialon in the SHS process.

3.2. Hot-pressing of the Slag α-sialon powder

The densities of both Slag α-sialon and Chem α-sialon samples hot-pressed at different temperatures are shown in Fig. 2. For Slag α-sialon samples, the density increases rapidly above 1450 °C, and reaches 3.16 g/cm^3 at 1550 °C. It keeps almost constant at sintering temperatures above 1550 °C. The Chem α-sialon sample shows a similar trend in densification to that of the Slag α-sialon, but its density is higher at 1450 °C and slightly lower above 1550 °C compared to the Slag α-sialon.

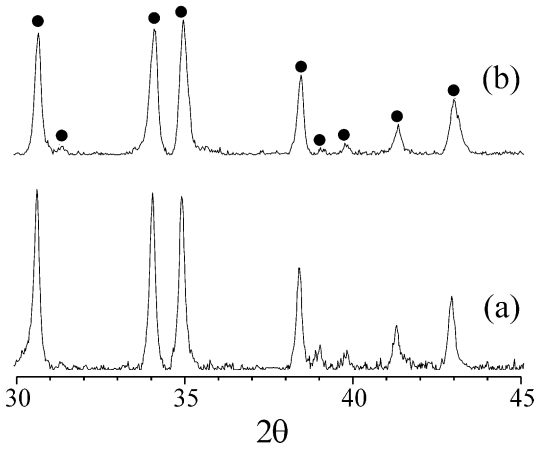

Fig. 1. XRD patterns of (a) Slag α-sialon and (b) Chem α-sialon powders derived by SHS (• α-sialon).

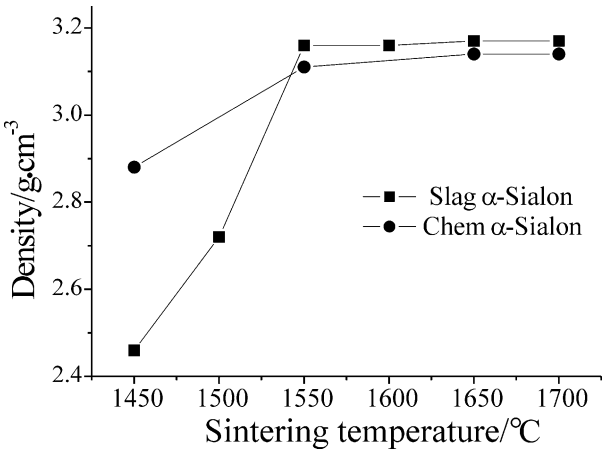

Fig. 2. Densities of Slag α-sialon and Chem α-sialon samples sintered at different temperatures.

This result indicates that the densification process for both samples has been completed around 1550 °C. The densities are 3.17 and 3.14 g/cm^3 for the two samples sintered at 1700 °C, respectively. The densification of SHS-ed α-sialons relies on the existence of a glassy phase in the samples. The softening of the glassy phase led to significant shrinkage occurred above 1450 °C for both samples.

SHS is a very rapid heating and cooling process. The reaction temperature could rapidly reach above 2000 °C and reaction could cease within seconds. Synthesis of α-sialon by SHS under a high nitrogen pressure is a complex process and involves thermal explosion, and gas- and liquid-phase reactions. Because the SHS combustion process yields very high temperature, the reactants involved are in liquid or gaseous state inside the combustion chamber and they could react very rapidly. All these conditions could lead to a meta-stable Slag α-sialon phase to form[1]. According to results by Rosenflanz and Chen[18] and by Shen[19] that α-sialon may persist as a meta-stable phase in systems where thermodynamic equilibrium varies with temperature and when the true thermodynamic equilibrium is kinetically retarded. The results of XRD analysis of Slag α-sialon samples are listed in Table 2. As shown, α-sialon is the main crystalline phase appeared in the entire sintering process, but a small amount of β-sialon appears when sintering temperature is above 1500 °C. When the Slag α-sialon powder was hot-pressed at 1450 °C, α-sialon was maintained as the only crystalline phase. It was noticed that the XRD peaks for β-sialon shifted slightly towards the higher 2θ value, i.e. decreasing in the d spacing, when temperatures increased from 1500 to 1700 °C, suggesting a decrease in the Al–O solubility in β-sialon with increase in temperature.

Previous studies[20,21] on α-sialon doped by rare-earth ions showed that α-sialon to β-sialon phase transformation could occur during heat treatment between 1200

Table 2
Phase assemblages and cell dimensions of Slag α-sialon samples sintered at different temperatures

Samples	Phase assemblages[a]	Cell dimensions of α- sialon	
		a(Å)	*c*(Å)
HP1450	α′/s	7.825 (1)	5.696 (1)
HP1500	α′/s, β′/w	7.827 (1)	5.696 (1)
HP1550	α′/s, β′/w	7.823 (1)	5.694 (1)
HP1600	α′/s, β′/w	7.820 (1)	5.693 (1)
HP1650	α′/s, β′/m	7.820 (1)	5.694 (1)
HP1700	α′/s, β′/m	7.818 (1)	5.691 (1)
HP1650[b]	α′/s, β′/m	7.818 (1)	5.688 (2)

[a] α′ = α-sialon, β′ = β-sialon, s = strong, m = medium, w = weak.
[b] Hot-pressed sample using Slag α-sialon powder plus La_2O_3 as starting materials.

Table 3
Phase assemblages and cell dimensions of Chem α-sialon samples sintered at different temperatures

Sample	Phase assemblages[a]	Cell dimensions of α′		Cell dimensions of β′	
		a(Å)	*c*(Å)	*a*(Å)	*c*(Å)
Powder	α′/s	7.824 (1)	5.692 (1)	–	–
HP1450	α′/s, β′/m, A/vw	7.825 (1)	5.689 (1)	7.702 (2)	2.988 (1)
HP1550	β′/s, α′/ms, A/vw	7.824 (1)	5.684 (1)	7.684 (1)	2.969 (2)
HP1650	β′/s, α′/w, A/vw	7.824 (1)	5.657 (2)	7.661 (1)	2.949 (1)
HP1550[b]	β′/s, α′/ms, A/vw	7.823 (1)	5.685 (1)	7.681 (1)	2.968 (1)

[a] α′ = α-sialon, β′ = β-sialon, s = strong, m = medium, vw = very weak, A = AlN-polytypoids.
[b] Hot-pressed sample using Chem α-sialon plus La_2O_3 as starting materials.

and 1500 °C, especially in α-sialon systems stabilized by light rare earth elements. These observations suggest that some α-sialon phases formed at elevated temperatures (~1800 °C) could be thermodynamically unstable at temperatures lower than the initial forming temperature and would transform to the more stable β-sialon phase. In contrast, Ca-α-sialon is found very stable,[22] and does not transform to β-sialon even after heat-treatment at 1450 °C for 200 h.[23] The stability of (Ca,Mg)-α-sialon has not been studied yet.

The starting material in the present work is the SHS-ed α-sialon powder. The stabilizing cations (Ca, Mg) in Slag α-sialon phase could be re-distributed through a dissolution–diffussion-precipitation process during sintering when a sufficient amount of liquid phase exists. The appearance of small amount of β-sialon phase in Salg α-sialon ceramics implies that more amount of Ca, Mg would de-dissolve from α-sialon phase to glassy phase when the sample was sintered at certain high temperature, thus resulting in the formation of β-sialon (see discussion in next section). This analysis is in consistence with the fact that the cell dimensions of the Slag α-sialon phase decreases with the increasing temperature, indicating the decrease in the $Ca(Mg)^{2+}$ concentration in the α-sialon phase (Table 2).[16] The decrease of α-sialon cell size has been found in accompaniment with the destabilization of Ca α-sialon phases.[23]

To investigate the cause of meta-stability of SHS-ed powder at elevated temperature, the contents of some elements in powder before and after SHS process were analyzed by ICP-AES technique. The results indicate that the ratios of Ca^{2+}:Mg^{2+}:Al^{3+} are 37.40:7.35:100 and 19.23:3.83:100 for the starting powder mixture (i.e. before SHS) and the powder after SHS process respectively, implying that there is serious loss of Ca^{2+} and Mg^{2+} during SHS process, which could be caused by evaporation of these compounds (CaO, MgO) at elevated temperatures. Most of Ca^{2+} and Mg^{2+} remained were incorporated into α-sialon for the balance of electric charge during SHS process, and restrained in α-sialon lattice during cooling down. Slag α-sialon phase decomposes into β-sialon could occur by reacting with the liquid phase and giving more stabilizing cations (Ca, Mg) into liquid phase above 1500 °C.

3.3. Hot-pressing of the Chem α-sialon powder

As shown in Fig. 1, the density of Chem α-sialon sample sintered at 1450 °C is higher than that of Slag α-sialon sample. It is understood that there were more impurities in the SHS-ed Slag α-sialon than in the SHS-ed Chem α-sialon, which could result in more glassy phases in the final Slag α-sialon product. However, the Chem α-sialon phase appeared less stable and partially decomposed at 1450 °C (Table 3) when the Slag α-sialon was still relatively stable (Table 2). The decomposition would follow the reaction $\alpha' + \text{Liquid}_1 \rightarrow \beta' + \text{Liquid}_2$.[24] Liquid phase 2 would contain more Ca^{2+} and Mg^{2+} than Liquid phase 1 due to the $\alpha' \rightarrow \beta'$ phase transformation and the amount of liquid phase in the sample would increase as well. An increased amount of Ca^{2+}/Mg^{2+}-containing liquid phase would contribute a higher density for Chem α-sialon at 1450 °C. This can also explain why the amount of glassy phase in the two samples sintered at 1700 °C appeared similar although there was less impurity in the stoichiometrical Chem α-sialon compositions than in the Slag α-sialon. With further increase in sintering temperature above 1550 °C, the difference in the densification behaviour of the two samples appeared very small. XRD analysis of Chem α-sialon samples hot-pressed at different temperatures is shown in Table 3, The phase assemblages consist of α-sialon, β-sialon and a small amount of AlN-polytypoid. The amount of β-sialon markedly increased with the increase of hot-pressing temperature above 1450 °C. On the other hand, the unit cell dimensions of α-sialon phase decreased with sintering temperature. In comparison with Slag α-sialon, the β-sialon contents in the

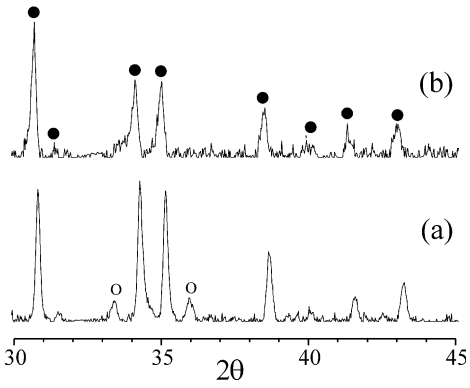

Fig. 3. XRD patterns of (a) Slag α-sialon and (b) Slag α-sialon + Slag samples sintered at 1650 °C (• α-sialon ○ β-sialon).

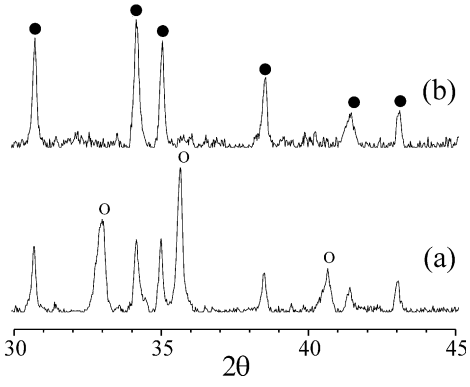

Fig. 4. XRD patterns of (a) Chem α-sialon and (b) Chem α-sialon + $CaCO_3$ samples hot-pressed at 1550 °C (• α-sialon ○ β-sialon).

Chem α-sialon samples sintered at different temperatures are all higher than that in the corresponding Slag α-sialons. Although the compositions for both Slag/Chem α-sialon SHS synthesis are calculated based on stoichiometry without any extra oxide additive, the instability of the Slag/Chem α-sialon may suggest an insufficient stabilizer in the starting composition as discussed above.

3.4. Effect of addition of cations on the phase assemblages of hot-pressed samples

Based on the above understanding, extra 10 wt.% slag and $CaCO_3$(CaO) were added into the Slag α-sialon and Chem α-sialon compositions respectively. XRD patterns of Slag α-sialon with additional slag and Chem α-sialon with additional $CaCO_3$ samples sintered at the different temperatures are shown in Figs. 3 and 4, respectively. For a comparison, the figures also include the XRD patterns of the parent samples with no extra Ca-bearing additives. As seen from Figs. 3 and 4, β-sialon phase disappears and the phase assemblages of both sintered samples consist of only α-sialon phase. As described above, in reaction of $\alpha' + \text{Liquid}_1 \rightarrow \beta' + \text{Liquid}_2$, Liquid 1 contains less amount of Ca^{2+}/Mg^{2+} than that in Liquid 2. The added extra slag and $CaCO_3$ respectively to Slag/Chem α-sialon powders could supply CaO and/or MgO in Liquid 1, restraining the shift of composition from α-sialon single-phase region to α-sialon/β-sialon two-phase region, and the formation of β-sialon, thus stabilizing α-sialon structure. The results of cell dimensions of α-sialon phase in hot-pressed both Slag/Chem α-sialon samples using addition of slag/$CaCO_3$ as starting materials are listed in Table 4.

3.5. Microstructure of hot-pressed samples with the addition of La_2O_3

Figs. 5 and 6 are the SEM photographs and EDS patterns of hot-pressed Slag and Chem α-sialon samples with the addition of La_2O_3, respectively. In order to know the influence of addition of La_2O_3 on the phase assemblages of Slag/Chem α-sialon samples, the results of XRD analysis before and after addition was compared. As listed in Tables 2 and 3, there is no obvious change on phase assemblages of hot-pressed samples and cell dimensions of α-sialon phase before and after the addition of La_2O_3. Thus the SEM observation on the samples by addition of La_2O_3 might reflect, to some extent, the microstructure. Grains of different morphologies, namely equi-axed, elongated (grains with relatively low aspects ratios) and needle-like (grains with relatively high aspect ratios), are seen in both the photographs. By EDS analysis, as shown in Figs. 5(b) and (c) and 6 (b) and (c), it has been found that α-sialon phase possesses both equi-axed and elongated morphologies. Because of the light cations-doped in (Ca,Mg)-α-sialon, it is difficult to distinguish α-sialon and β-sialon phases from the back-scattered SEM mode

Table 4
Phase assemblages and cell dimensions of Slag/Chem α-sialon samples with and without addition of slag and $CaCO_3$ as starting materials

Starting powders	Hot-pressing temperature (°C)	Phase assemblages[a]	Cell dimensions of α′	
			a(Å)	c(Å)
Slag α-sialon	1650	α′/s, β′/m	7.820 (1)	5.694 (1)
Slag α-sialon plus slag		α′/s	7.818 (1)	5.691 (1)
Chem α-sialon	1550	β′/s, α′/ms, A/vw	7.824 (1)	5.684 (1)
Chem α-sialon plus $CaCO_3$		α′/s	7.818 (1)	5.689 (2)

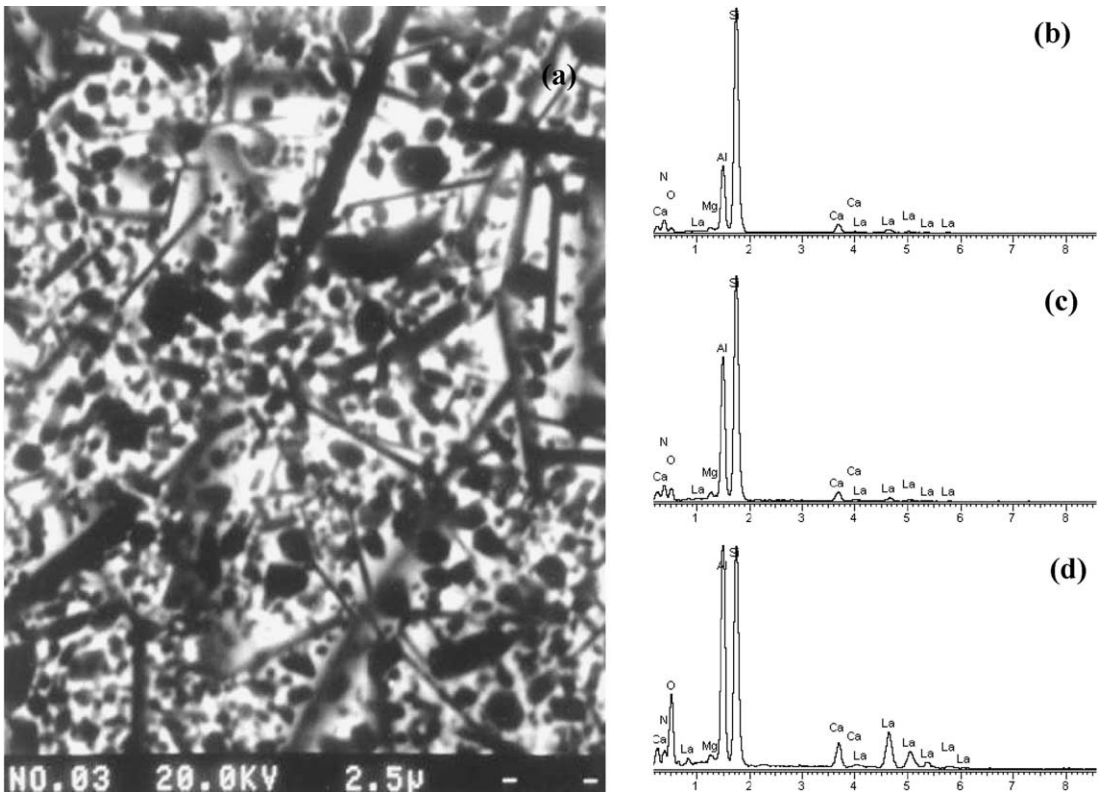

Fig. 5. Microstructure photographs of hot-pressed Slag α-sialon samples with the addition of La_2O_3 at the mode of back-scattered electron (a) microstructural photograph (b) EDS pattern of equi-axed grains (c) EDS pattern of elongated grains (d) EDS pattern of grain boundary phase.

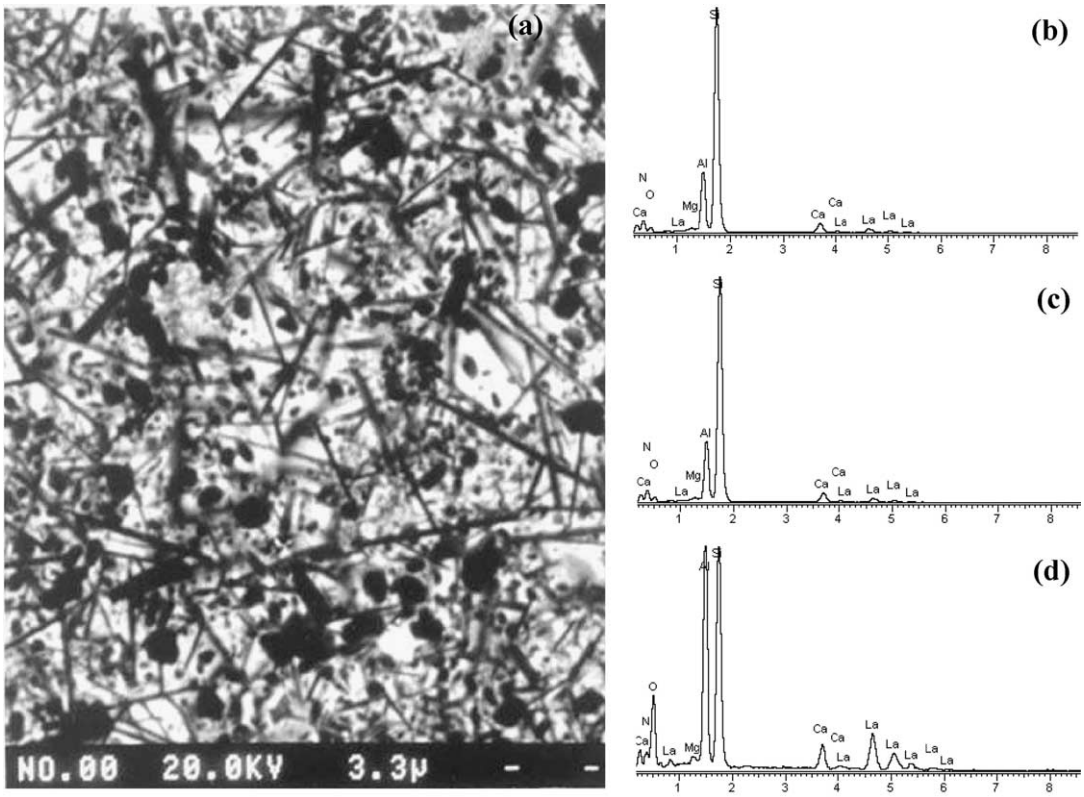

Fig. 6. Microstructure photographs of hot-pressed Chem α-sialon samples with the addition of La_2O_3 at the mode of back-scattered electron (a) microstructural photograph (b) EDS pattern of equi-axed grains (c) EDS pattern of elongated grains (d) EDS pattern of grain boundary phase.

[see Figs. 5(a) and 6(a)]. However, it is thought that grains with the needle-like morphology in Figs. 6(a) and 5(a) are β-sialon, as reported by literature.[25,26]

The areas with white color in Figs. 5(a) and 6(a) are grain boundary glassy phase containing La, as supported by EDS patterns in Figs. 5(d) and 6(d). It is also noted that La atom appears in the α-sialon grains, as seen in Figs. 5(b) and (c) and 6(b) and (c), with amount of much less than that in grain boundary.

4. Conclusions

SHS technology can be used to synthesize α-sialon powder from both stoichiometrical compositions and some industrial wastes through proper selection of composition. α-sialon synthesized by SHS is densified through liquid sintering mechanism, and could decompose to form β-sialon during hot-pressing at 1500 °C and above, whose amount increases with sitering temperature. However, the addition of extra Ca^{2+} into the SHS-ed α-sialon powder could improve the stability of the α-sialon phases. Enlogated α-sialon grains could be obtained in hot-pressed slag α-sialon materials.

Acknowledgements

This work was supported by The Outstanding Overseas Chinese Scholars Fund of Chinese Academy of Sciences and National Natural Sciences Foundation of China.

References

1. Chen, W. W., Wang, P. L., Chen, D. Y., Zhang, B. L., Jiang, J. X., Cheng, Y. B. and Yan, D. S., Synthesis of (Ca,Mg) α-sialon from slag by Self-propagating high-temperature synthesis. *J. Mater. Chem.*, 2002, **12**, 1199–1202.
2. Ekström, T. and Nygren, M., Sialon ceramics. *J. Am. Ceram. Soc.*, 1992, **75**(2), 259–276.
3. Narciso, F. J. and Rodriguez-Reinoso, F., Synthesis of β-sialon from clays: effect of starting materials. *J. Mater. Chem.*, 1994, **7**, 1137–1141.
4. Ekström, T., Shen, Z., Mackenzie, K. J. D., Brown, I. W. M. and White, G. V., α-Sialon ceramics synthesized from a clay precursor by carbothermal reduction and nitridation. *J. Mater. Chem.*, 1998, **8**, 977–983.
5. Higgins, I. and Hendry, A., Production of β-sialon by carbothermal reduction of Kaolinite. *Br. Ceram. Trans. J.*, 1986, **85**, 161–166.
6. Hrabe, Z., Komarneni, S., Malla, P., Srikanth, V. and Roy, R., Pillared montmorillonite clay as a raw material for the synthesis of β-sialon. *J. Mater. Sci.*, 1992, **27**, 4614–4618.
7. Merzhanov, A. G. and Borovinskaya, I. P., Self-propagating High temperature Synthesis of Refractory Inorganic compounds. *Dokl. Chem.*, 1972, **204**, 429–432.
8. Yi, H. C. and Moore, J. J., Review: Self-propagating high-temperature (combustion) synthesis (SHS) of powder-compacted materials. *J. Mater.Sci.*, 1990, **25**, 1159–1168.
9. Jiang, G. J., Zhuang, H. R., Li, W. L., Wu, F. Y., Zhang, B. L. and Fu, X. R., Mechanisms of combustion synthesis of aluminum nitride in high pressure nitrogen atmosphere (2). *J. Mater. Synth. Process*, 1999, **7**, 1–6.
10. Chen, K. X., Jin, H. B., Zhou, H. P. and Ferreira, J. M. F., Combustion synthesis of AlN–SiC solid solution particles. *J. Eur. Ceram. Soc.*, 2000, **20**, 2601–2606.
11. Miyamoto, Y., Kanehira, S., Hirota, K. and Yamaguchi, O., Development of recycling process for industrial wastes by SHS. *Int. J. SHS*, 2000, **9**, 357–362.
12. Kaolio, M., Ruuskanen, P., Maki, J. and Läthteenmäki, S., Use of the aluminothermic reaction in the treatment of steel industry by-products. *J. Mater. Syn. Proc*, 2000, **8**, 87–92.
13. Miyamoto, Y. and Tanihata, L. Z., Recycling processes of Si wastes to advanced ceramics using SHS reaction. *Ann. Chim. Fr*, 1995, **20**, 197–203.
14. Jack, K. H., Review: Sialon and related nitrogen ceramics. *J. Mater. Sci.*, 1976, **11**, 1135–1158.
15. Johansson, K. E., Palm, T. and Werner, P. E., An automatic microdensitometer for X-ray diffraction photographs. *J. Phys. E.: Sci. Instrum.*, 1980, **13**, 1289–1291.
16. Wang, P. L., Li, Y. W. and Yan, D. S., Effect of dual elements (Ca,Mg) and (Ca, La) on cell dimensions of multi-cation α-sialon. *J. Eur. Ceram. Soc.*, 2000, **20**, 1333–1337.
17. Wang, P. L., Li, Y. W. and Yan, D. S., Effect of amount and atomic ratio of dual modifiers Ca and Mg phase formation and mechanical properties of Ca,Mg-α-Sialons. *J. Mater. Sci.*, 2000, **35**, 1585–1588.
18. Rosenflanz, A. and Chen, I. W., Phase relationship and stability of α-Sialon. *J. Am. Ceram. Soc.*, 1999, **82**, 1025–1036.
19. Shen, Z. J., Ekström, T. and Nygren, M., Temperature stability of samarium-doped α-sialon ceramics. *J. Eur. Ceram. Soc.*, 1996, **16**, 43–53.
20. Shen, Z. and Nygren, M., Nd-doped α-Sialon and related phase: stability and compatibility. *Mater. Sci. Forum.*, 2000, **325-326**, 191–198.
21. Mandal, H., Thompson, D. P. and Ekström, T., Reversible α↔β Sialon transformation in heat-treated sialon ceramics. *J. Eur. Ceram. Soc.*, 1993, **12**, 421–429.
22. Mandal, H. and Thompson, D. P., α↔β Sialon transformation in calcium-containing α-sialon ceramics. *J. Eur. Ceram. Soc.*, 1999, **19**, 543–552.
23. Hewett, C. L., Cheng, Y. B., Muddle, B. C. and Trigg, M. B., Thermal stability of calcium α-sialon ceramics. *J. Eur. Ceram. Soc.*, 1998, **18**, 417–427.
24. Zhao, R. P. and Cheng, Y. B., Decomposition of Sm α-sialon phases during post-sintering heat treatment. *J. Am. Ceram. Soc.*, 1996, **16**, 1001–1008.
25. Drew, P. and Lewis, M. H., The microstructures of silicon nitride ceramics during hot-pressing transformations. *J. Mater. Sci.*, 1974, **9**, 261–269.
26. Lange, F. F., Fracture toughness of Si_3N_4 as a function of initial α-phase content. *J. Am. Ceram. Soc.*, 1979, **62**(7–8), 428–430.